THE GEOLOGICAL SOCIETY OF AMERICA®

Time scales of magma transport and mixing at Kīlauea Volcano, Hawai'i

Auriol S.P. Rae[1]*, Marie Edmonds[1], John Maclennan[1], Daniel Morgan[2], Bruce Houghton[3], Margaret E. Hartley[1], and Isobel Sides[1]
[1]Department of Earth Sciences, University of Cambridge, Cambridge CB2 3EQ, UK
[2]School of Earth and Environment, University of Leeds, Leeds LS2 9JT, UK
[3]Department of Geology and Geophysics, University of Hawai'i at Mānoa, Honolulu, Hawaii 96822, USA

ABSTRACT

Modeling of volcanic processes is limited by a lack of knowledge of the time scales of storage, mixing, and final ascent of magmas into the shallowest portions of volcanic plumbing systems immediately prior to eruption. It is impossible to measure these time scales directly; however, micro-analytical techniques provide indirect estimates based on the extent of diffusion of species through melts and crystals. We use diffusion in olivine phenocrysts from the A.D. 1959 Kīlauea Iki (Hawai'i, USA) eruption to constrain the timing of mixing events in the crustal plumbing system on time scales of months to years before eruption. The time scales derived from zonation of Fe-Mg in olivines, combined with contemporaneous geophysical data, suggest that mixing occurred on three time scales: (1) as much as 2 yr prior to eruption in the deep storage system; (2) in a shallow reservoir, between incoming hot melts and resident melt for several weeks to months prior to eruption; and (3) in the conduit and summit reservoir, between the resident magma and cooled surface lava, draining back into the vent on time scales of hours to several days during pauses between episodes. Synchronous inflation of the shallow reservoir with deep earthquake swarms and mixing suggests an intermittently open transcrustal magmatic system.

INTRODUCTION

Determining the time scales of pre-eruptive and syn-eruptive magmatic processes is a primary objective of modern volcanology. Time scales of magma movement through the lithosphere prior to eruptions are difficult to resolve unequivocally with geophysical techniques, yet understanding these time scales is critical for eruption forecasting. Swarms of earthquakes at a range of depths often occur prior to eruptions and are inferred to be caused by magma movement. It has not been possible to state with certainty whether these earthquakes are linked with the magma that eventually erupts. However, the chemistry and microtextures of crystals may be used as rate meters of magma mixing (e.g., Costa et al., 2009; Kahl et al., 2011; Martin et al., 2008; Ruprecht and Plank, 2013). Analysis of the chemical stratigraphy of crystals, using time scales from diffusion chronometry (e.g., Costa et al., 2003, 2008, 2009; Costa and Chakraborty, 2004; Costa and Dungan, 2005; Morgan et al., 2004; Morgan and Blake, 2005; Nakamura, 1995), provides constraints on magma ascent rates and crystal residence times that may be compared with contemporaneous geophysical data acquired prior to and during a volcanic eruption (e.g., Kahl et al., 2013).

We apply this method to the 1959 eruption of Kīlauea Iki, Kīlauea Volcano, Hawai'i, USA (Fig. 1), the type example of a powerful Hawaiian fountaining eruption. It included the highest fountaining ever observed at Kīlauea (Richter et al., 1970) and was the first eruption at Kīlauea that was rigorously geophysically monitored (Eaton and Murata, 1960; Eaton et al., 1987). The magma budget is well estimated by tilt measurements (Eaton et al., 1987), direct observation (Richter et al., 1970), and geochemical studies (Helz, 1987; Anderson and Brown, 1993; Sides et al., 2014). The eruption presents an excellent opportunity to retrospectively constrain the timing of magma ascent and mixing with respect to eruption triggering. It was preceded by significant seismicity and ground deformation linked to magma movement (Eaton et al., 1987) and involved 17 episodes of eruption (Richter et al., 1970). Geophysical and geochemical observations suggest that magma stored in a shallow reservoir was mixed, during and between episodes, with primitive magmas from depth as well as with cooler, outgassed lava that had drained back from a lava lake formed in episode 1 (Murata and Richter, 1966; Richter and Murata, 1966; Wright, 1973; Eaton et al., 1987; Helz, 1987; Loewen, 2013; Sides et al., 2014).

Our aim is to constrain the timing of magma mixing events prior to and during the A.D. 1959 eruption of Kīlauea Iki through the characterization of Mg-Fe zonation in olivine crystals. These time scales are then compared with the timings of deformation and seismicity recorded during the eruption. We seek to understand time scales of magma storage and transport to better constrain our understanding of the significance of seismic swarms that traverse the mantle and crust prior to eruptions at Kīlauea Volcano.

METHOD

When a crystal, in equilibrium with a melt, experiences a change in intrinsic parameters of

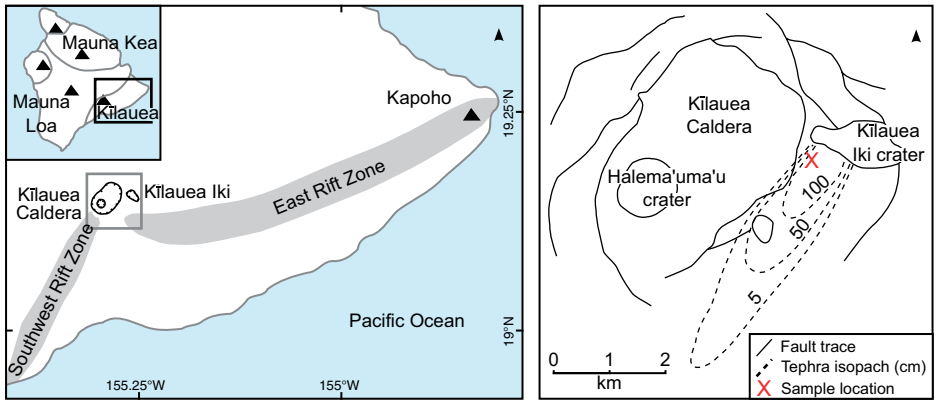

Figure 1. The location of the Kīlauea Iki crater and samples (for details, see the Data Repository [see footnote 1]). Based on Sides et al. (2014) and Stovall et al. (2010).

*Current address: Department of Earth Science and Engineering, Imperial College London, London SW7 2BP, UK; Email: a.rae14@imperial.ac.uk.

TABLE 1. MODELING PARAMETERS

Episode	Temperature (°C)		Oxygen fugacity (ΔNNO)		Pressure (kbar)
	Low	High	Low	High	
1	1190 ± 10	1259 ± 10	–1.7 (Roeder et al., 2003)	–0.5 (Gerlach, 1993)	1 ± 1 (Poland et al., 2014)
3	1117 ± 10–1160 ± 10	1264 ± 10–1287 ± 10			
5	1153 ± 10–1161 ± 10	1250 ± 10–1282 ± 10			
8	1147 ± 10–1170 ± 10	1235 ± 10–1279 ± 10			
10	1180 ± 10	1310 ± 10			
15	1140 ± 10–1160 ± 10	1256 ± 10–1292 ± 10			

Note: Each crystal was assigned temperature conditions independently; the ranges indicate the minimum and maximum temperature by episode. NNO—Ni-NiO buffer.

the host magma (e.g., pressure, temperature, or composition), the system's chemistry will respond to re-approach equilibrium conditions. If the crystal remains at conditions such that significant diffusion of a particular element is possible, then over time the composition profile of that element at the crystal boundary will relax, creating a smoothed compositional profile whose shape reflects the diffusivity of the element and the relaxation time (Costa and Morgan, 2011). In principle, it is possible to estimate the time elapsed since the change in intrinsic parameters using the geometry of the diffusion profile (Costa and Morgan, 2011) and a diffusion coefficient. For Fe-Mg in olivine, the coefficient of diffusion is dependent upon temperature, oxygen fugacity, pressure, composition, and crystallographic orientation. By comparing the measured composition profile to a set of profiles with specific initial and boundary conditions, assuming a diffusion coefficient, a time scale can be determined between the mixing-transport event and quenching (e.g., Hartley et al., 2016). We use high-resolution backscatter images of 70 crystallographically oriented olivine crystals from 6 episodes of the 1959 eruption. Profiles along 44 olivines were calibrated for Fe-Mg composition by electron probe microanalysis. Of these, 24 compositional profiles reconstructed from backscatter images were used for diffusion chronometry modeling. Several of the 24 modeled profiles had more than one compositional zone; therefore, 29 diffusional zones were modeled. For full details of the samples, methods, and uncertainties, see the GSA Data Repository[1].

The profiles were modeled using temperatures calculated by using the Mg thermometer for matrix glass (Helz and Thornber, 1987) and temperatures calculated to be in equilibrium with olivine core compositions. These temperatures provide upper and lower bounds, unique to each crystal, on the temperature (Table 1; see the Data Repository). The oxygen fugacity (f_{O_2}) of the system was assumed to be $\Delta\log f_{O_2} = -1.7$, relative to the Ni-NiO (NNO) buffer (Roeder et al., 2003); however, using a higher oxygen fugacity of $\Delta\log f_{O_2} = -0.5$, relative to the NNO buffer (Gerlach, 1993), reduces the time scales by a factor of ~1.6. This uncertainty is small compared to the uncertainty due to temperature.

RESULTS

The composition of the olivine cores is typically more magnesium (forsterite, Fo) rich than the rim, i.e., they are normally zoned. Olivine cores typically contain ~87 mol% Fo but range between 82.7 and 88.2 mol% Fo. Rim and intermediate compositions are more variable, from 80 to 88 mol% Fo, with a broad peak at ~82.5 mol% Fo. There is a paucity of olivine compositions of 84–86 mol% Fo (Fig. 2).

Figure 3 shows the ages of mixing events as determined from diffusion chronometry for crystals from the six studied episodes of the eruption. The compositional zones may be divided into distinct populations: 15 crystals displayed a single normal zone formed from –600 days; 6 crystals had broad reverse zones (although 2 of these were not modeled due to the effects of nonuniform initial composition), formed from –450 days, and 4 of these had a much narrower normal zone at the crystal rim, formed in <31 days. The remaining three crystals displayed complex zonation patterns with a large range of time scales. Some crystals displayed very thin (<3 μm wide) deviations from the modeled profiles at the crystal rim, likely to represent the eruptive quench event; these were not modeled. Later episodes contain a larger proportion of crystals with more than one diffusional zone and, within these, the youngest zone (at the rim of the crystal) always corresponds to times close to or after the beginning of the eruption.

The time scales calculated from diffusion modeling using the temperatures calculated to be in equilibrium with the olivine cores are approximately one-third of those calculated using the temperatures from the glass compositions. The inferred ages are shown in Figure 4 along with contemporaneous geophysical data and a schematic diagram of the plumbing system beneath Kīlauea Volcano. The crystals record mixing events up to ~–820 days. Mixing events became increasingly frequent toward the eruption onset; 50% of the mixing events occurred from ~–50 days onward. Mixing took place quasi-continuously during the 35 days of eruption, generating both reverse and normal zoning.

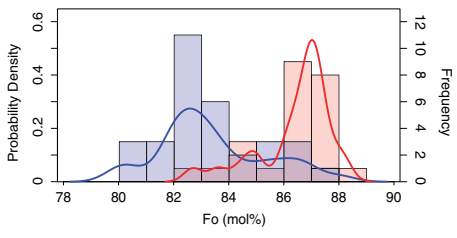

Figure 2. Compositional data of studied olivines. Red—olivine core compositions (n = 24), blue—olivine rim and intermediate zone compositions (n = 29). Raw data are plotted as histograms binned at every 1 mol% Fo. Probability density curves are shown as solid lines.

DISCUSSION

The distribution of compositions of the olivine cores and rims, combined with the zoning patterns, suggests a complex petrogenetic history for the crystal cargo of this eruption. The wide range of olivine core compositions (Fig. 2) has been linked to crystal mush disaggregation supplying primitive olivines, with fractionation during shallow storage producing the olivines with the lower Fo cores (Clague et al., 1995).

There are several possible causes of the zonation identified here. In all crystals diffusion acts due to disequilibrium across the crystal face, thus the diffusion is caused by changes in the intrinsic properties of temperature, pressure, oxygen fugacity, and/or melt composition. Of these, temperature and melt composition are most significant for changing the equilibrium chemistry of olivine (Roeder and Emslie, 1970; Ford et al., 1983). Cooling, or a decrease in MgO content, causes normal zoning while sub-liquidus heating, or an increase in MgO content, causes reverse zoning.

Approximately 60% of the mixing events recorded by the olivines took place after the onset of shallow (<10 km) seismicity (Fig. 4). The number of mixing events increases rapidly with time up to the eruption onset, paralleling the increasing frequency of upper crustal seismicity from 50 events/day initially to more than 1000 events/day by –14 days (Eaton et al., 1987). The mixing events and seismicity in the upper crust over the few weeks prior to eruption plausibly represent the intrusion of melts from depth into a shallow summit reservoir. We are unable to distinguish between the south caldera and Halema'uma'u reservoirs as the location of mixing, but it is clear that magmas were hosted, albeit briefly, and mixed in one of the reservoirs.

[1]GSA Data Repository item 2016153, methods, Tables DR1–DR4 (operating conditions and compositional data), Figures DR1–DR3, electron microprobe data and electron backscattered diffraction data (Summary.xlsx), and calibrated compositional profiles, and their derivation from greyscale profiles calibrated with electron microprobe data (Profiles.xlsx), is available online at www.geosociety.org/pubs/ft2016.htm, or on request from editing@geosociety.org or Documents Secretary, GSA, P.O. Box 9140, Boulder, CO 80301, USA.

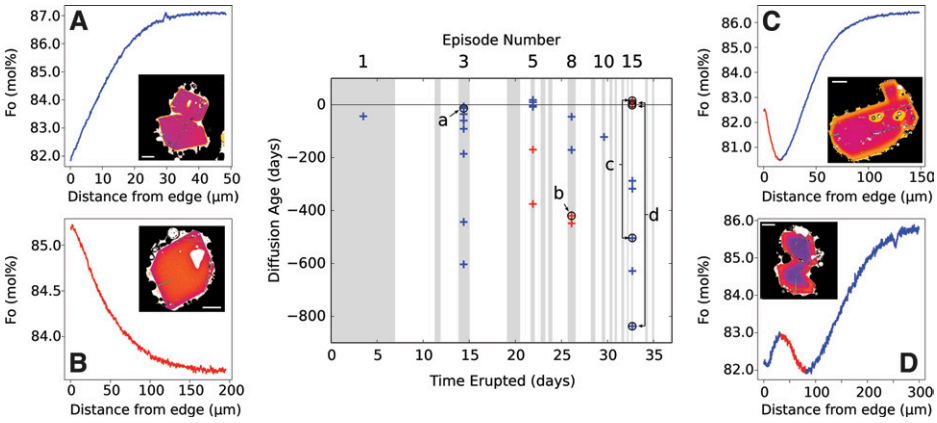

Figure 3. The time that each crystal erupted versus the diffusion ages (using glass temperatures) of each zone. The onset time of the eruption = 0. Blue points correspond to normal zones; red points correspond to reverse zones. Gray bars indicate the timings of each of the episodes of the 1959 eruption. Circled points correspond to plots (a–d) showing the compositional profiles that produced the time scales indicated alongside false-color backscatter images. The white scale bars are 250 μm in length, and the green lines indicate the location of the profile.

Approximately 40% of the mixing events recorded by the olivines occurred before the onset of shallow seismicity (Fig. 4). During this time period, summit tilt meters recorded quasi-continuous inflation and sporadic deep (45–65 km) swarms of earthquakes (as much as 600 days before eruption) were recorded. This period was marked by an absence of shallow seismicity (Eaton et al., 1987). Although these old zones may reflect mixing during the steady inflation of the summit, there is a period of time, from –350 to –150 days, with no measured inflation. We suggest that the old mixing events, before –150 days, could be associated with the deep seismic swarms recorded at 45–65 km depth. The old zones include both normal and reverse zones, implying the mixture of different composition and/or temperature melts, each bearing their own crystal cargoes, i.e., a hot, mantle-derived, MgO-rich magma bearing high-Fo olivines mixing with cooler, MgO-poor magmas bearing low-Fo olivines. Although the deep earthquake swarms cannot be linked individually to any particular magma mixing event as recorded in the olivine, there is a suggestion that mixing occurred sporadically at depth, associated with seismicity, prior to the Kīlauea Iki eruption. The time scales calculated here are consistent with estimates of time scales between melt segregation from the mantle and eruption based on U-series disequilibria suggesting a maximum of 7 yr (Girard et al., 2012). It is critical, however, that the shallow magma reservoir beneath the summit exhibited periods of inflation from –800 to –350 days, and from –150 days until the eruption (Eaton et al., 1987). This suggests that deep intrusions were supplying magma via an open system (generating little seismicity) throughout this period. This analysis implies that the time scales for magma ascent from 45 to 65 km depth might be significantly less than 800 days and may be as short as weeks to months. These short time scales would be consistent with other studies showing rapid ascent of magmas from mantle depths to the surface (Ruprecht and Plank, 2013). Furthermore, the occurrence of deep swarms of earthquakes after the start of the eruption might indicate that magmas were drawn up from depth on the time scale of the eruption, similar to the downward-propagating seismicity observed during the Eyjafjallajokull (Iceland) eruption in 2010 (Tarasewicz et al., 2012).

The volume of magma intruded into the shallow reservoir declined as the eruption continued (to near zero by episode 8; Eaton et al., 1987), while drainback volumes remained fairly constant throughout the eruption. Several of the diffusion zones indicate mixing events after episode 8; it therefore seems likely that these zones were formed as a result of mixing between the magma in the shallow reservoir and the drainback lava, which may have driven further vesiculation and new episodes of fountaining. The return of drained-back lavas to the shallow storage reservoir is supported by melt inclusion geochemistry (Sides et al., 2014; Wallace and Anderson, 1998).

This study provides the first geochemical constraint on the time scales of magma residence and mixing through the mantle and crust

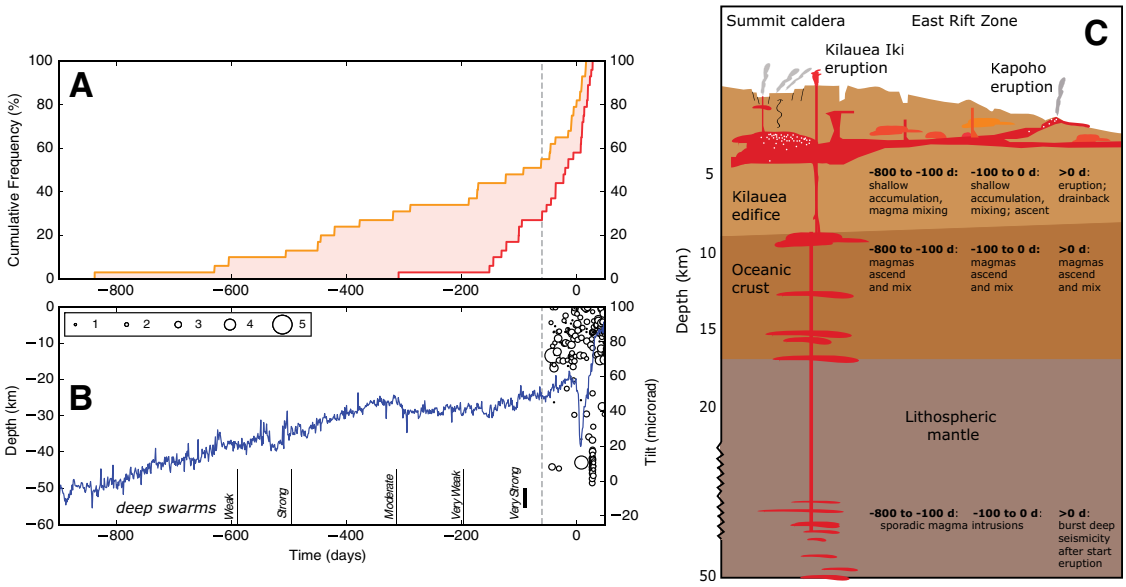

Figure 4. A: Ages of olivine diffusion zones, displayed as a cumulative frequency plot with time. Orange and red lines correspond to the distributions derived from minimum (glass) and maximum (olivine) temperatures, respectively. The vertical dashed line indicates the onset of shallow seismicity. B: Records of radial tilt (from the Uwekahuna tilt meter) and earthquake depths and sizes recorded by the seismic network around Kīlauea Volcano (Eaton et al., 1987). Earthquake data show focal depths and, where possible, magnitudes. Sensitive short-period telemetered seismometers were installed 150 days before the eruption. Prior to that installation, earthquakes were detected but their locations were less precise. The vertical black bars indicate the locations of deep earthquake swarms, duration (width), and strength as described by Eaton et al. (1987). C: Schematic illustration of the magmatic plumbing system of Kīlauea and its relation to the timings of mixing events.

at Kīlauea. The 1959 Kīlauea Iki eruption was triggered by magma mixing in the shallow crust, synchronous with shallow seismicity in the weeks leading up to the eruption. Mixing occurred up to 800 days before eruption, consistent with the timing of sporadic swarms of deep earthquakes, which probably mark the intrusion of mantle-derived melts into the deep Kīlauea plumbing system. Magmas migrated up into the shallow system rapidly and quasi-continuously during the ~2 yr preceding the eruption. Approximately 60% of the mixing events analyzed took place <100 days prior to and during the eruption, caused by magma movement in the upper crust and by drainback processes during the eruption. The link to the deep mantle was maintained even after the start of the eruption.

ACKNOWLEDGMENTS

We acknowledge Natural Environment Research Council studentship funds (Sides) and a U.S. Geological Survey (USGS) Jack Kleinman grant, which allowed samples for this study to be collected. Don Swanson (USGS) provided invaluable advice in the field. Rae gratefully acknowledges M. Kahl for several valuable discussions. We thank M. Poland, N. Vinet, M. Rhodes, and four anonymous reviewers for their detailed and constructive comments.

REFERENCES CITED

Anderson, A.T., and Brown, G.G., 1993, CO_2 contents and formation pressures of some Kilauean melt inclusions: American Mineralogist, v. 78, p. 794–803.

Clague, D.A., Moore, J.G., Dixon, J.E., and Friesen, W.B., 1995, Petrology of submarine lavas from Kilauea's Puna Ridge, Hawaii: Journal of Petrology, v. 36, p. 299–349, doi:10.1093/petrology/36.2.299.

Costa, F., and Chakraborty, S., 2004, Decadal time gaps between mafic intrusion and silicic eruption obtained from chemical zoning patterns in olivine: Earth and Planetary Science Letters, v. 227, p. 517–530, doi:10.1016/j.epsl.2004.08.011.

Costa, F., and Dungan, M., 2005, Short time scales of magmatic assimilation from diffusion modeling of multiple elements in olivine: Geology, v. 33, p. 837–840, doi:10.1130/G21675.1.

Costa, F., and Morgan, D.J., 2011, Time constraints from chemical equilibration in magmatic crystals, *in* Dosseto, A., et al., eds., Time scales of magmatic processes: Chichester, UK, John Wiley & Sons, p. 125–159.

Costa, F., Chakraborty, S., and Dohmen, R., 2003, Diffusion coupling between trace and major elements and a model for calculation of magma residence times using plagioclase: Geochimica et Cosmochimica Acta, v. 67, p. 2189–2200, doi:10.1016/S0016-7037(02)01345-5.

Costa, F., Dohmen, R., and Chakraborty, S., 2008, Time scales of magmatic processes from modeling the zoning patterns of crystals: Reviews in Mineralogy and Geochemistry, v. 69, p. 545–594, doi:10.2138/rmg.2008.69.14.

Costa, F., Coogan, L.A., and Chakraborty, S., 2009, The time scales of magma mixing and mingling involving primitive melts and melt-mush interaction at mid-ocean ridges: Contributions to Mineralogy and Petrology, v. 159, p. 371–387, doi:10.1007/s00410-009-0432-3.

Eaton, J.P., and Murata, K.J., 1960, How volcanoes grow: Science, v. 132, p. 925–938, doi:10.1126/science.132.3432.925.

Eaton, J.P., Richter, D.H., and Krivoy, H.L., 1987, Cycling of magma between the summit reservoir and Kīlauea Iki lava lake during the 1959 eruption of Kīlauea volcano (Hawaii), *in* Decker, R.W., et al., eds., Volcanism in Hawaii: Papers to commemorate the 75th anniversary of the founding of the Hawaiian Volcano Observatory: U.S. Geological Survey Professional Paper 1350, p. 1307–1335.

Ford, C.E., Russell, D.G., Craven, J.A., and Fisk, M.R., 1983, Olivine-liquid equilibria: Temperature, pressure and composition dependence of the crystal/liquid cation partition coefficients for Mg, Fe2+, Ca and Mn: Journal of Petrology, v. 24, p. 256–266, doi:10.1093/petrology/24.3.256.

Gerlach, T.M., 1993, Oxygen buffering of Kīlauea volcanic gases and the oxygen fugacity of Kīlauea basalt: Geochimica et Cosmochimica Acta, v. 57, p. 795–814, doi:10.1016/0016-7037(93)90169-W.

Girard, G., Reagan, M.K., Sims, K.W., Garcia, M.O., Pietruszka, A.J., and Thornber, C.R., 2012, From mantle to ash cloud: Quantifying magma generation, ascent, and degassing rates at Kilauea during short-lived explosive episodes using short-lived U-series radionuclide disequilibria: American Geophysical Union Fall Meeting 2012, abs. V13D–2884.

Hartley, M.E., Morgan, D.J., Maclennan, J., Edmonds, M., and Thordarson, T., 2016, Tracking time scales of short-term precursors to large basaltic fissure eruptions through Fe-Mg diffusion in olivine: Earth and Planetary Science Letters, v. 439, p. 58–70, doi:10.1016/j.epsl.2016.01.018.

Helz, R.T., 1987, Diverse olivine types in lava of the 1959 eruption of Kīlauea volcano and their bearing on eruption dynamics, *in* Decker, R.W., et al., eds., Volcanism in Hawaii: Papers to commemorate the 75th anniversary of the founding of the Hawaiian Volcano Observatory: U.S. Geological Survey Professional Paper 1350, p. 691–722.

Helz, R.T., and Thornber, C.R., 1987, Geothermometry of Kīlauea Iki lava lake, Hawaii: Bulletin of Volcanology, v. 49, p. 651–668, doi:10.1007/BF01080357.

Kahl, M., Chakraborty, S., Costa, F., and Pompilio, M., 2011, Dynamic plumbing system beneath volcanoes revealed by kinetic modeling, and the connection to monitoring data: An example from Mt. Etna: Earth and Planetary Science Letters, v. 308, p. 11–22, doi:10.1016/j.epsl.2011.05.008.

Kahl, M., Chakraborty, S., Costa, F., Pompilio, M., Liuzzo, M., and Viccaro, M., 2013, Compositionally zoned crystals and real-time degassing data reveal changes in magma transfer dynamics during the 2006 summit eruptive episodes of Mt. Etna: Bulletin of Volcanology, v. 75, p. 1–14, doi:10.1007/s00445-013-0692-7.

Loewen, M.W., 2013, Volatile mobility of trace metals in volcanic systems [Ph.D. thesis]: Corvallis, Oregon State University, 217 p.

Martin, V.M., Morgan, D.J., Jerram, D.A., Caddick, M.J., Prior, D.J., and Davidson, J.P., 2008, Bang! Month-scale eruption triggering at Santorini Volcano: Science, v. 321, p. 1178–1178, doi:10.1126/science.1159584.

Morgan, D.J., and Blake, S., 2005, Magmatic residence times of zoned phenocrysts: Introduction and application of the binary element diffusion modelling (BEDM) technique: Contributions to Mineralogy and Petrology, v. 151, p. 58–70, doi:10.1007/s00410-005-0045-4.

Morgan, D.J., Blake, S., Rogers, N.W., DeVivo, B., Rolandi, G., Macdonald, R., and Hawkesworth, C.J., 2004, Time scales of crystal residence and magma chamber volume from modelling of diffusion profiles in phenocrysts: Vesuvius 1944: Earth and Planetary Science Letters, v. 222, p. 933–946, doi:10.1016/j.epsl.2004.03.030.

Murata, K.J., and Richter, D.H., 1966, Chemistry of lavas of the 1959–1960 eruption of Kilauea volcano, Hawaii: U.S. Geological Survey Professional Paper 537-A, 26 p.

Nakamura, M., 1995, Residence time and crystallization history of nickeliferous olivine phenocrysts from the northern Yatsugatake volcanoes, central Japan: Application of a growth and diffusion model in the system Mg-Fe-Ni: Journal of Volcanology and Geothermal Research, v. 66, p. 81–100, doi:10.1016/0377-0273(94)00054-K.

Poland, M.P., Miklius, A., and Montgomery-Brown, E.K., 2014, Magma supply, storage, and transport at shield-stage Hawaiian volcanoes, *in* Poland, M.P., et al., eds., Characteristics of Hawaiian volcanoes: U.S. Geological Survey Professional Paper 1801, p. 179–234, doi:10.3133/pp18015.

Richter, D.H., and Murata, K.J., 1966, Petrography of the lavas of the 1959–1960 eruption of Kilauea volcano, Hawaii: U.S. Geological Survey Professional Paper 537-D, 12 p.

Richter, D., Eaton, J., Murata, K., Ault, W., and Krivoy, H., 1970, Chronological narrative of the 1959–1960 eruption of Kilauea volcano, Hawaii: U.S. Geological Survey Professional Paper 537-E, 73 p.

Roeder, P.L., and Emslie, R.F., 1970, Olivine-liquid equilibrium: Contributions to Mineralogy and Petrology, v. 29, p. 275–289, doi:10.1007/BF00371276.

Roeder, P.L., Thornber, C., Poustovetov, A., and Grant, A., 2003, Morphology and composition of spinel in Pu'u 'O'o lava (1996–1998), Kīlauea volcano, Hawaii: Journal of Volcanology and Geothermal Research, v. 123, p. 245–265, doi:10.1016/S0377-0273(02)00508-5.

Ruprecht, P., and Plank, T., 2013, Feeding andesitic eruptions with a high-speed connection from the mantle: Nature, v. 500, p. 68–72, doi:10.1038/nature12342.

Sides, I., Edmonds, M., Maclennan, J., Houghton, B.F., Swanson, D.A., and Steele-MacInnis, M.J., 2014, Magma mixing and high fountaining during the 1959 Kīlauea Iki eruption, Hawai'i: Earth and Planetary Science Letters, v. 400, p. 102–112, doi:10.1016/j.epsl.2014.05.024.

Stovall, W.K., Houghton, B.F., Gonnermann, H., Fagents, S.A., and Swanson, D.A., 2010, Eruption dynamics of Hawaiian-style fountains: The case study of episode 1 of the Kīlauea Iki 1959 eruption: Bulletin of Volcanology, v. 73, p. 511–529, doi:10.1007/s00445-010-0426-z.

Tarasewicz, J., Brandsdóttir, B., White, R.S., Hensch, M., and Thorbjarnardóttir, B., 2012, Using microearthquakes to track repeated magma intrusions beneath the Eyjafjallajökull stratovolcano, Iceland: Journal of Geophysical Research, v. 117, B00C06, doi:10.1029/2011JB008751.

Wallace, P.J., and Anderson, A.T., 1998, Effects of eruption and lava drainback on the H_2O contents of basaltic magmas at Kīlauea Volcano: Bulletin of Volcanology, v. 59, p. 327–344, doi:10.1007/s004450050195.

Wright, T.L., 1973, Magma mixing as illustrated by the 1959 eruption, Kilauea Volcano, Hawaii: Geological Society of America Bulletin, v. 84, p. 849–858, doi:10.1130/0016-7606(1973)84<849:MMAIBT>2.0.CO;2.

Manuscript received 16 February 2016
Revised manuscript received 20 April 2016
Manuscript accepted 20 April 2016

Printed in USA